ELSEVIER

15 August 1999

Optics Communications 167 (1999) 283–290

OPTICS COMMUNICATIONS

www.elsevier.com/locate/optcom

Full length article

2.8 μm Er:YLF laser transversely pumped with a CW diode laser bar

Mark Tikerpae *, Stuart D. Jackson, Terence A. King

Laser Photonics Group, Department of Physics and Astronomy, Schuster Laboratory, The University of Manchester, Manchester, M13 9PL, UK

Received 16 March 1999; received in revised form 10 June 1999; accepted 15 June 1999

Abstract

We present experimental results on the operation of a 1 cm diode bar-side-pumped Er:YLF laser. The mid-infrared laser produced a maximum average output power of 51 mW (102 mW peak power) for 3.1 W of chopped (50% duty cycle) pump power. When operated in true CW mode, 16 mW output power was recorded for a total pump power of 4.0 W. The centre wavelength of the spectral output of the laser was measured to be 2721 nm $\pm$ 5 nm. The threshold pump power and slope efficiency of the Er:YLF laser were measured as a function of the diode laser centre wavelength and the laser cavity length. Measurements of the spatial beam profile indicated TEM_{00} operation.

PACS: 42.55.Xi; 42.55.Rz; 42.60.Pk; 42.60.Lh
Keywords: Transverse-pumped; Diode-pumped; Mid-IR; Er:YLF

1. Introduction

The $^4I_{11/2} \rightarrow {}^4I_{13/2}$ transition of Er^{3+}, with a wavelength in the region of 2.7–3.0 μm, has been investigated in a variety of Er^{3+} doped crystal lasers with diode laser excitation [1–3]. Such diode pumped lasers would become efficient and compact tools in medicine because of the strong absorption by water of light at these wavelengths [4].

Until now, work on the diode pumped Er:YLF laser has almost exclusively involved end-pumped configurations due to the relatively high slope efficiency and low threshold pump power that is possible with such a geometry and achieving over 1 W of output power [5,6]. 1 W of CW output power has also been achieved from a diode laser end-pumped Er:YAG laser [7]. It is desirable that lasers be constructed without the use of sophisticated pump optics because of the reduced cost and complexity. Transversely pumped lasers, at the expense of efficiency as compared to end-pumping, could ultimately offer high average powers because of the high pump powers that are provided by diode bars or arrays.

* Corresponding author. Tel.: +44-161-275-4292; fax: +44-161-275-4293; e-mail: markt@fs4.ph.man.ac.uk

0030-4018/99/$ - see front matter
PII: S0030-4018(99)00320-X

The optimum pump wavelength for Er^{3+} doped crystal lasers for operation on the $^4I_{11/2} \rightarrow {}^4I_{13/2}$ transition has been established to be approximately 970 nm [1]. Light at this wavelength directly excites the upper laser level, increasing the Stokes efficiency and consequently reducing the losses arising from thermal effects. The absorption coefficient is higher for a pump wavelength of 970 nm compared to that of 790 nm and the combined effects of two upconversion processes and a cross-relaxation process present in Er:YLF, are optimised for efficient laser operation at the longer pump wavelength [8,9].

To our knowledge only pulsed operation has been reported previously from a transversely pumped Er:YLF laser which was pumped with a quasi-CW (QCW) diode laser [10]. This communication describes the operation of a CW side-pumped Er:YLF laser with the beam profile, beam divergence and output wavelength characterised. In addition, the slope efficiency and the threshold pump power for laser operation has been investigated as a function of the diode laser centre wavelength and cavity geometry and the optimum configuration established.

2. Experimental arrangement

Fig. 1 shows the experimental arrangement of the transversely pumped Er:YLF laser. The Er:YLF crystal (Spectragen, IL) had dimensions of $1.8 \times 4.0 \times 9$ mm and the doping concentration of the crystal was 15% Er^{3+}, optimised for pumping at a wavelength of 970 nm [5]. The Er:YLF laser crystal was placed directly onto a Peltier effect thermo-electric cooler (TEC) device. The planar back face of the crystal was coated (Rocky Mountain Instrument, Colorado) for high reflection at a wavelength of 2.8 μm, and formed the back mirror of the laser cavity, whilst the opposite face was coated for anti-reflection at a wavelength of 2.8 μm. The pump face at the side of the crystal was polished but not anti-reflection coated. The geometry of the crystal was such that the polarisation of the pump laser beam was parallel to the *a* axis of the crystal. The output coupler (Laseroptik, Germany) was 99% reflecting at the laser wavelength and had a radius of curvature (ROC) of 150 mm. In general we were limited by the low optical quality of a number of output couplers and hence the results below relate to the use of only one output coupler.

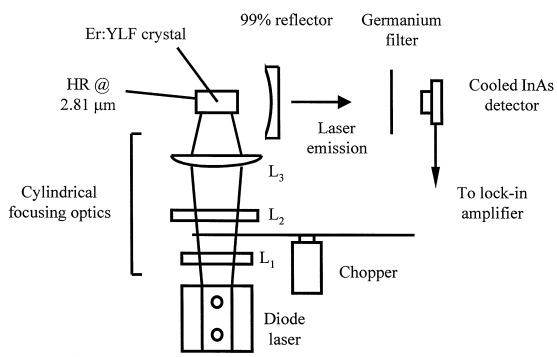

Fig. 1. Experimental arrangement of the side pumped Er:YLF laser. $L_1 = 12$ mm focal length, $L_2 = 40$ mm focal length, $L_3 = 40$ mm focal length.

The diode laser (Opto Power, OPC-A020-975-CS) was a 1 cm bar that could emit up to 20 W of power at a drive current of 35 A, depending on junction temperature. At the output power level used in these experiments the spectral bandwidth (FWHM) of the diode laser bar was approximately 2.5 nm, although this increased to 3.5 nm when operated at the maximum power of 20 W. The divergence (FWHM) was 11.5° in the horizontal plane and 48.6° in the vertical plane. The diode laser was mounted on a copper block cooled with a TEC device mounted on a water-cooled copper heat sink. The vertical plane of the diode laser emission was collimated and focused with two cylindrical lenses with focal lengths of 12 and 40 mm, respectively. The horizontal plane of the diode emission was focused into the crystal with a cylindrical lens, of focal length 40 mm. In this plane, the pump beam displayed some spatial structure originating from the individual emitters. In the vertical plane the pump beam could be focused down to 200 μm (FWHM). At the focus, the width of the pump beam was smaller than the cavity mode (measured to have a diameter of approximately 400 μm at the $1/e^2$ point), although the diode laser exhibited a degree of 'smile' (a bowing of the ray bundle due to sagging in the diode laser substrate) which became significant, relative to the spot size, at a distance along the pump axis of only 2 or 3 mm from the focus. Fig. 2 shows the calculated attenuation and the measured beam profile, of the focused pump laser, through the laser crystal and the overlap with

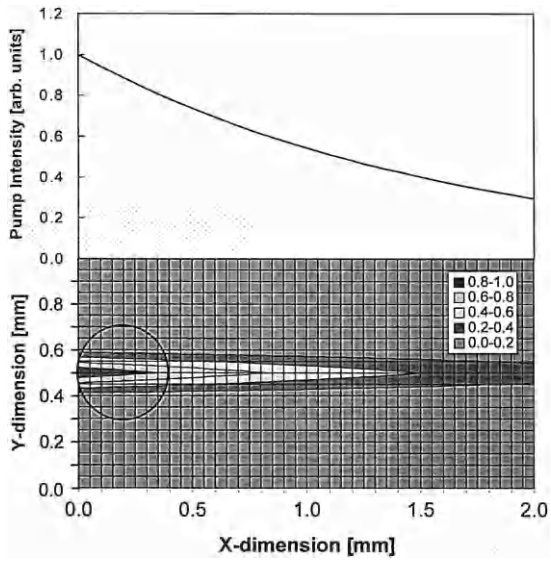

Fig. 2. Attenuation of the pump laser through the laser medium and contour map of the pump intensity through the crystal as viewed along the resonator axis. The circle represents the cross-section of the resonator mode.

the cavity mode. The location of the cavity mode shown corresponds to the maximum possible amount of pump absorption within the mode volume, although diffractive losses from the crystal edge probably force the cavity mode to be shifted slightly further inside the crystal for maximum efficiency. Approximately 90% of the incident light was absorbed by the laser crystal and a maximum of 21% of the incident pump power was absorbed within the laser mode. A chopper was placed between the diode laser and the Er:YLF crystal for repetitive pulse operation.

In order to separate the Er:YLF laser output from stray pump light, the beam was filtered with a polished slice of germanium (cut-off wavelength at 1.9 μm). A cooled InAs detector was used in conjunction with a Princeton lock-in amplifier to detect the 2.8 μm fluorescence. A calibrated power meter was used to measure the output power from the laser. Measurements of the spectral profile of the Er:YLF laser were performed using a monochromator with a resolution of 1.5 nm.

3. Results

The average output power of the side pumped Er:YLF laser as a function of average pump power is shown in Fig. 3. True CW operation and QCW operation (where the pump beam was chopped at a repetition rate of 35 Hz and with a duty cycle of 50%) are both shown. The maximum power for QCW operation was 51 mW (corresponding to a peak power of 102 mW), with the polarisation parallel to the crystal *c* axis, for an average pump power of 3.1 W (6.2 W peak pump power). This was the pump power incident upon the crystal pump face.

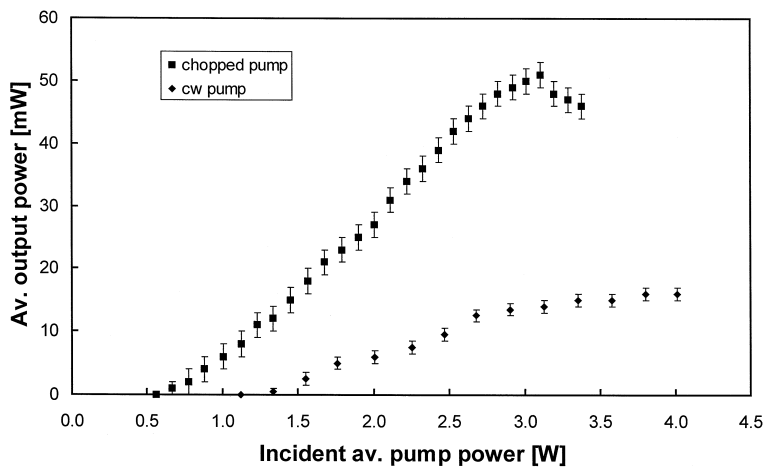

Fig. 3. Power output as a function of average pump power for the CW and the QCW laser.

The slope efficiency in this configuration was 2.5% and the threshold pump power was 560 mW. In the true CW case, the maximum power measured was 16 mW for a pump power of 4.0 W. Higher pump powers were not attempted due to the danger of fracture due to thermally induced stress. The slope efficiency was only 1% but the threshold pump power was 1120 mW, which corresponds to the same peak power as for QCW operation. The low slope efficiency of the CW laser was measured even at low pump powers of 1.5 W, so that the thermal problems associated with the QCW laser at average pump powers of 3.1 W and higher probably do not cause the reduced slope efficiency in the CW case. Alternative explanations for this behaviour are currently being sought. In addition, within the experimental error, the output in the CW case did not increase for pump powers greater than 3.5 W.

The observed drop in output power at pump powers greater than 3.1 W (for the QCW case) could be attributed to diffractive losses at the edge of the laser crystal resulting from the increase in the size of the cavity mode due the thermal lens effect. Crystalline YLF has a negative value for $\mathrm{d}n/\mathrm{d}T$ (-4.3×10^{-6} K^{-1} for π-polarisation in Nd:YLF [11]) which produces a negative thermal lens, of focal length, f, when lasers based on this material are significantly pumped. The focal length of the thermally induced lens for a slab-like medium in the direction normal to the plane of the incident pump light is given by [12]:

$$f = \frac{1}{2L}\left[\frac{\mathrm{d}n}{\mathrm{d}T}\left(\frac{Q}{2K}\right) - \frac{Q\alpha E B_{\perp}}{(1-\upsilon)K}\right]^{-1}, \qquad (1)$$

where L is the length of the slab, Q is the rate of heat deposited per unit volume, K is the thermal conductivity (0.06 W cm^{-1} K^{-1}), α is the thermal coefficient of expansion (8×10^{-6} K^{-1}), E is the Young's modulus (7.65×10^{5} kg/cm^2), $B_{\perp}$ is the photoelastic coefficient for the crystal axis perpendicular to the polarisation, and ν is Poisson's ratio (0.33) [12]. A value for the rate of heat deposited per unit volume, Q, was determined by multiplying the fraction of the total pump power (3.1 W) that was absorbed within the cavity mode volume with the quantum defect of the laser ($\lambda_{\mathrm{pump}}/\lambda_{\mathrm{laser}} = 0.35$). Regions outside of the cavity mode volume were not considered in this approximation. The focal length of the induced lens within the gain volume was calculated to be approximately -26 cm, using the appropriate pump and cavity parameters of the laser (such as the length of the slab, 9 mm, the cavity mode radius, 200 μm, and the resonator length, 12 mm). This was done for focusing relating to refractive index changes due to the temperature gradient only, because the photoelastic coefficients of YLF were unknown. The stress induced focusing would partially compensate for the thermally induced lens because the stress component creates a positive lens.

An ABCD ray tracing program was used to calculate the cavity mode radius at the back mirror as a function of the focal length of the thermally induced lens. It was established that when the focal length of the lens becomes shorter than approximately -25 cm, the cavity mode waist displays a significant increase in size. For a focal length of -26 cm, for the thermally induced lens, the cavity mode waist increases in size by approximately 23%. As the focal length of the thermal lens shortens further, it has been calculated that the increase in cavity mode size is dramatic, more than doubling for a thermally induced lens with a focal length of -15 cm, explaining the sudden drop in output power. This indicates that the drop in output power is almost certainly due to diffractive losses arising from the thermal lens effect. In comparison Jensen et al. [5] measured a drop in slope efficiency for a pump power of approximately 8 W. Using the cavity parameters described, a thermal lens of focal length -4 cm was calculated for their configuration. Using the ABCD ray tracing program it was calculated that for the configuration used the cavity mode should start to become unstable for a thermal lens of focal length shorter than approximately -4 cm. The reasons for the reduced sensitivity to the input power in this case are the reported increased pump mode volume and the shorter ROC output coupler.

The slope efficiency and the threshold pump power for the QCW laser, as a function of the diode laser centre wavelength, are shown in Fig. 4. The minimum threshold pump power for laser operation in this unoptimised configuration was 0.67 W when the pump centre wavelength was 973.3 nm. The absorption spectrum of the Er:YLF a axis shows that the greatest absorption is in the wavelength range of 972–973 nm [1]. It is expected that the threshold

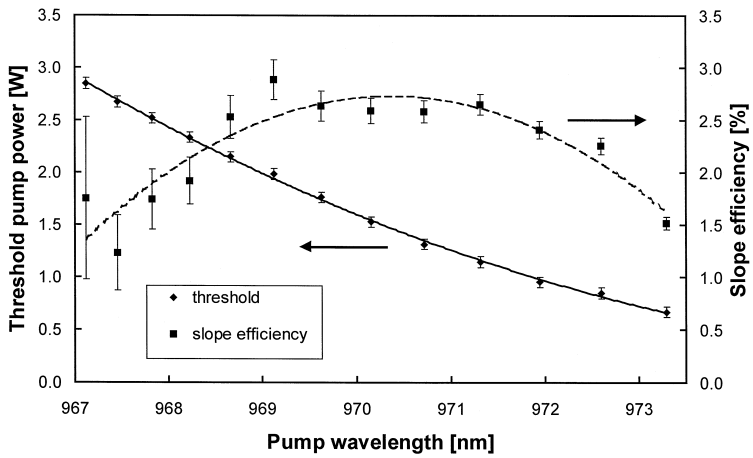

Fig. 4. Slope efficiency and threshold dependence on pump laser centre wavelength for the QCW laser.

pump power would decrease significantly at higher values of the absorption coefficient since more of the pump light is absorbed into the cavity mode volume, and this was measured to be the case. The highest values of the slope efficiency occur at pump wavelengths in the 969–972.5 nm range which overlaps with the maximum values of the broad features of the absorption spectrum of the Er:YLF *a* axis. The large errors associated with the measurements of the QCW slope efficiencies relate to the non-linearity of the output power curve as a function of the pump power, close to threshold (see Fig. 3 and Refs. [5,6]).

The QCW output power was measured as a function of the diode laser centre wavelength (Fig. 5), for a pump power of 2.8 W. The highest output power was measured for a pump wavelength of 972 nm. Whilst in previous work Stoneman et al. [13] have reported that the best performance from Ti:sapphire pumped Er:YLF was not obtained at the highest values of the material absorption coefficient (> 15 cm^{-1}), our results do not contradict this conclusion. Stoneman et al. [13] determined that with very high absorption coefficients and for *c* axis pumping, there was a drop in slope efficiency and an increase in the

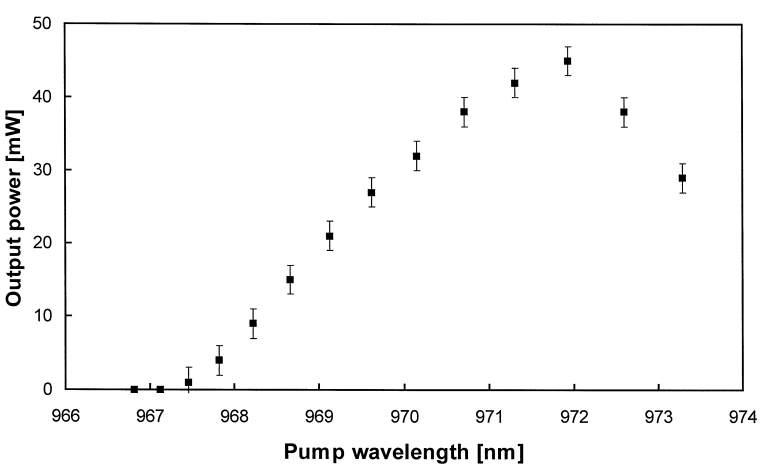

Fig. 5. Average QCW output power as a function of pump laser centre wavelength. Pump power = 2.8 W.

threshold pump power. This was attributed to upconversion from the upper laser level at high excitation rates per unit volume and, in addition, there is increased excited state absorption of the pump light from the upper laser level in regions of high excitation. However, at pump wavelengths where the absorption coefficient was lower than 15 cm^{-1} there was no discernible trend, except that for pumping on the *a* axis the threshold pump power decreased as the absorption coefficient increased from values of 5 to 12 cm^{-1}, agreeing with our measurements. The combination of the results from the two studies show that the optimum absorption coefficient lies in the region of 10–15 cm^{-1}. For most diode laser-pumped Er:YLF lasers the effective absorption coefficient experienced by the pump light rarely exceeds values of 10–12 cm^{-1} because of the broadened spectral bandwidth of the diode laser and the lower doping concentrations of approximately 15% Er^{3+}. Hence, the conclusions drawn from the results presented here are applicable to diode-pumped devices because upconversion from the upper laser level is significantly reduced.

The slope efficiency and the threshold pump power of the laser were measured as a function of the cavity mode radius (see Fig. 6). This was done by varying the length of the resonator. The pump wavelength during this experiment was fixed at 972 nm and the pump laser beam was chopped. The threshold is lowest and the slope efficiency greatest for the smallest mode radius, of 190 μm, within the laser crystal. The intracavity photon intensity is greatest for the smallest cavity mode radius, hence achieving the greatest rate of stimulated emission from the gain volume. The highest output power achieved, for 3.0 W average pump power, was with the shortest cavity length and the output power dropped off as the cavity length (and hence the mode radius) increased.

The spectral profile of the QCW Er:YLF laser is shown in Fig. 7. The laser was operated with a pump power of 3.5 W so that there was approximately 750 mW absorbed into the laser mode volume and the output power was 35 mW. The main emission peak is centred on 2721 nm ± 5 nm, the main part of the error deriving from the systematic uncertainty on the measurement of the absolute wavelength. There is some structure to the peak that could not be clearly resolved by the monochromator (which had a resolution of 1.5 nm). In addition, there is a lower intensity peak at 2668 nm. At high pump powers only, a third intensity peak was detected at 2814 nm but was unstable and disappeared altogether at lower pump powers. The longer wavelength line (2814 nm) has been measured to be dominant in our unpublished end-pumping experiments where more pump light was absorbed into the cavity mode volume. It has been suggested that the main transition in the Er:YLF laser is between the second Stark level of $^4I_{11/2}$ and the fourth Stark level of $^4I_{13/2}$ [8]. The calculated wavelength of the transition between these Stark levels is 2809 nm roughly corresponding to the third

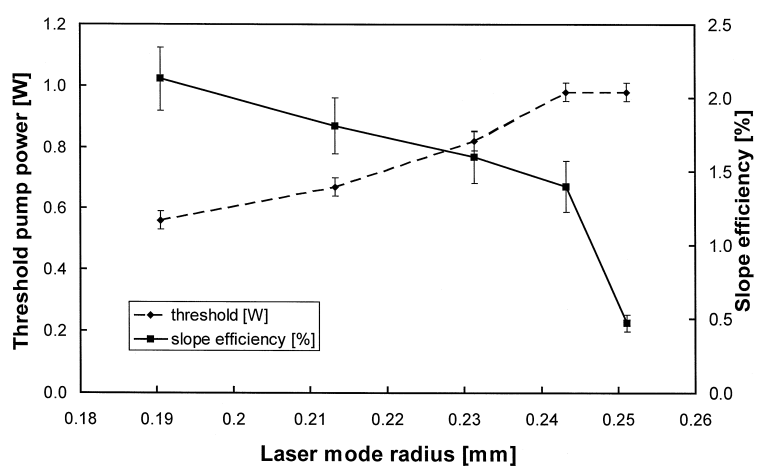

Fig. 6. Slope efficiency and threshold dependence on resonator length for the QCW laser.

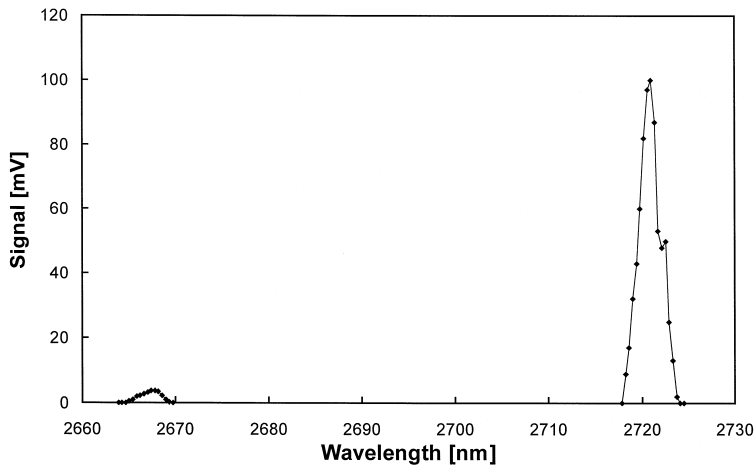

Fig. 7. Spectral profile of the QCW side pumped Er:YLF laser.

intensity peak measured, based upon values of 10 232 cm^{-1} and 6672 cm^{-1} for the wavenumber of these energy levels [14,15].

Longer emission wavelengths have been observed to dominate as the absorbed pump power is increased in Er:BaY_2F_8 [16]. This behaviour of the spectral output of the 2.8 μm Er^{3+} laser can be understood by calculating the relative gain of competing transitions between Stark level pairs [17]. The population inversion for each transition can vary because of the way in which the total population density of a manifold is distributed amongst the Stark levels as determined by the Boltzmann distribution. As the pump intensity increases, the lower laser level becomes more heavily populated and transitions terminating into the lowest lying Stark levels of the lower laser manifold are quenched because these levels contain most of the total population density. In this way, only longer wavelength transitions are supported at higher pump intensities.

The spatial profile of the transversely pumped Er:YLF laser was measured, when operated at an average output power of 35 mW in the QCW mode and with a cavity length of 12 mm. The spatial profile was determined to be close to Gaussian in both the horizontal and vertical planes, indicating TEM_{00} operation. From the results of measurements of the spot size (measured at the point where the intensity dropped to $1/e^2$ of its peak value), the half-angle divergence of the laser was determined to be 5.5 mrad in the horizontal plane and 5.0 mrad in the vertical plane.

This laser system has the potential for some optimisation. Pumping the stronger absorption of the *c* axis would increase the absorbed pump power without increasing the absolute power and thermal load on the crystal. Investigations are continuing to improve the pump optics to optimise the spatial overlap of the pump beam and the cavity mode by reducing hotspots in the beam and to fill the cavity mode more efficiently. Alternative resonator configurations are also being considered to alleviate the problems associated with the thermally induced lens. In addition, measurements using higher quality output couplers will be undertaken to characterise the effect of changing the reflectivity of the optic and its ROC.

4. Conclusions

An Er:YLF side-pumped slab laser has been constructed and pumped with a 1 cm diode laser bar. The main spectral line of the laser was measured to be centred at 2721 nm ± 5 nm and the divergence 5.5 mrad. The slope efficiency and threshold has been measured for both QCW and CW operation. The performance of the laser was superior in the QCW system and an average output power of 51 mW was achieved. Thermally induced lensing caused

the output power to decrease at pump powers greater than 3.1 W by increasing the cavity mode size and introducing diffractive losses from the edge of the laser crystal. The slope efficiency and threshold were also measured as a function of pump wavelength and cavity length. At 2.8 W average pump power, the optimum pump wavelength was 972 nm coinciding with the peak absorption in Er:YLF. The laser performed best at short cavity lengths due to the reduction in cavity mode radius.

Acknowledgements

The support of the Engineering and Physical Sciences Research Council and Spectron Laser Systems is gratefully acknowledged.

References

[1] R.C. Stoneman, J.G. Lynn, L. Esterowitz, IEEE J. Quantum Electron. 28 (1992) 1041.
[2] B.J. Dinerman, P.F. Moulton, Opt. Lett. 19 (1994) 1143.
[3] M. Pollnau, W. Lüthy, H.P. Weber, T. Jensen, G. Huber, A. Cassanho, H.P. Jenssen, R.A. McFarlane, Opt. Lett. 21 (1996) 48.
[4] J. Boulnois, Lasers Med. Sci. 1 (1986) 47.
[5] T. Jensen, A. Diening, G. Huber, B.H.T. Chai, Opt. Lett. 21 (1996) 585.
[6] M. Pollnau, R. Spring, S. Wittwer, W. Lüthy, H.P. Weber, J. Opt. Soc. Am. B 14 (1997) 974.
[7] D.-W. Chen, C.L. Fincher, T.S. Rose, F.L. Vernon, R.A. Fields, Opt. Lett. 24 (1999) 385.
[8] M. Pollnau, Th. Graf, J.E. Balmer, W. Lüthy, H.P. Weber, Phys. Rev. A 49 (1994) 3990.
[9] M. Tikerpae, S.D. Jackson, T.A. King, J. Mod. Opt. 45 (1998) 1269.
[10] H. Voss, F. Massmann, OSA trends in Optics and Photonics Series 10, Advanced Solid State Lasers (1997) 217.
[11] T.M. Pollak, W.F. Wing, R.J. Grasso, E.P. Chicklis, H.P. Jenssen, IEEE J. Quantum Electron. 18 (1982) 159.
[12] W. Koechner, Solid-State Laser Engineering, 2nd ed., Springer Series in Optical Sciences, vol. 1, Springer-Verlag, 1988.
[13] R.C. Stoneman, J.G. Lynn, L. Esterowitz, IEEE J. Quantum Electron. 28 (1992) 1041.
[14] R.A. McFarlane, J. Opt. Soc. Am. B 8 (1991) 2009.
[15] M.V. Petrov, A.M. Tkachuk, Opt. Spectrosc. (USSR) 45 (1978) 81.
[16] S. Wittwer, M. Pollnau, R. Spring, W. Lüthy, H.P. Weber, R.A. McFarlane, Ch. Harder, H.P. Meier, Opt. Commun. 132 (1996) 107.
[17] V. Lupei, S. Geogescu, V. Florea, IEEE J. Quantum Electron. 29 (1993) 426.